Chapter 3

Eppley Pyranometer Thermal Offset Characterization

3.1 Origin of the Thermal Offset in Eppley Pyranometers

The thermal offset originates from a difference of temperature across the internal components of the instrument. Several authors [4], [13] have analyzed the theoretical behavior of the thermal offset. These analyses are based on the work of Philipona [24] on the pyrgeometer, an instrument with a similar design.

The domes of a PSP can be considered transparent to solar radiation and opaque to most of the infrared radiation [13]. The outer dome exchanges infrared radiation with the atmosphere, the outer space and the inner dome. The outer dome is considered to be nearly opaque in the IR wavelength. The inner dome also exchanges heat with the outer dome and the absorber.

The outer dome is usually colder than the body of the instrument and therefore colder than the inner dome, which in turn is colder than the absorber. This temperature gradient through the instrument can be attributed to the following reasons:

- The domes have a smaller heat capacity than the body of the instrument. It allows the domes to change temperature faster than the body and creates a temperature gradient in the instrument.
- The domes have a small thermal conductivity that creates a temperature gradient between the base and tip of the domes.
- The thermal conductivity between the body and the domes is further limited due to the contact resistance between the base of the domes and the body.
- The outer dome faces directly the sky and has a hemispherical IR emissivity of 0.9, which leads to strong radiative cooling.
- The domes are transparent to a large fraction of the solar spectum (0.3-2.5 μ m) whereas the body, although painted white, absorbs part of the solar radiation. The temperature gradient can therefore be greater during daytime than at night.
- The instrument remains in a transient thermal state because of continuous changes in the surface and air temperature, wind, fraction of cloud cover, precipitation and evaporation of dew.

The temperature gradient between the absorber and the inner dome produces a loss of energy from the absorber. This loss of energy is what creates the thermal offset.

Haeffelin et al [13] developed an analytical model of the energy balance of the pyranometer to relate the instrument temperatures to the instrument offset. In this analysis the heat flux arriving at the detector is defined as

$$F_{net} = \alpha_s \tau_d E + \alpha_s \varepsilon_d \sigma T_d^4 + \alpha_s \varepsilon_s \rho_d \sigma T_s^4 - \varepsilon_s \sigma T_s^4. \tag{3.1}$$

Equation 3.1 is derived from the energy balance on the detector of the PSP. The term ($\alpha_s\ \tau_d E$) corresponds to the solar irradiance E transmitted through the dome with a transmissivity τ_d and absorbed by the detector with an absorptivity α_s. The term ($\alpha_s\ \varepsilon_d\ \sigma T_d^4$) corresponds to the amount of radiation emitted by the dome with an emissivity ε_d at a temperature T_d and absorbed by the detector with an absorptivity α_s. The term ($\alpha_s\ \varepsilon_s\ \rho_d\ \sigma T_s^4$) represents the amount of radiation emitted by the detector with an emissivity ε_s at a temperature T_s, reflected by the dome with a reflectivity ρ_d and absorbed by the detector with an absorptivity α_s. The term ($\varepsilon_s\ \sigma T_s^4$) correspond to the amount of radiation emitted by the detector with an emissivity ε_s.

The Flux F_{net} can also be written as a function of the Seebeck coefficient of the thermopile and the voltage output of the thermopile as follows:

$$F_{net} = \frac{T_s - T_b}{C} = \frac{SU_e}{C}, \tag{3.2}$$

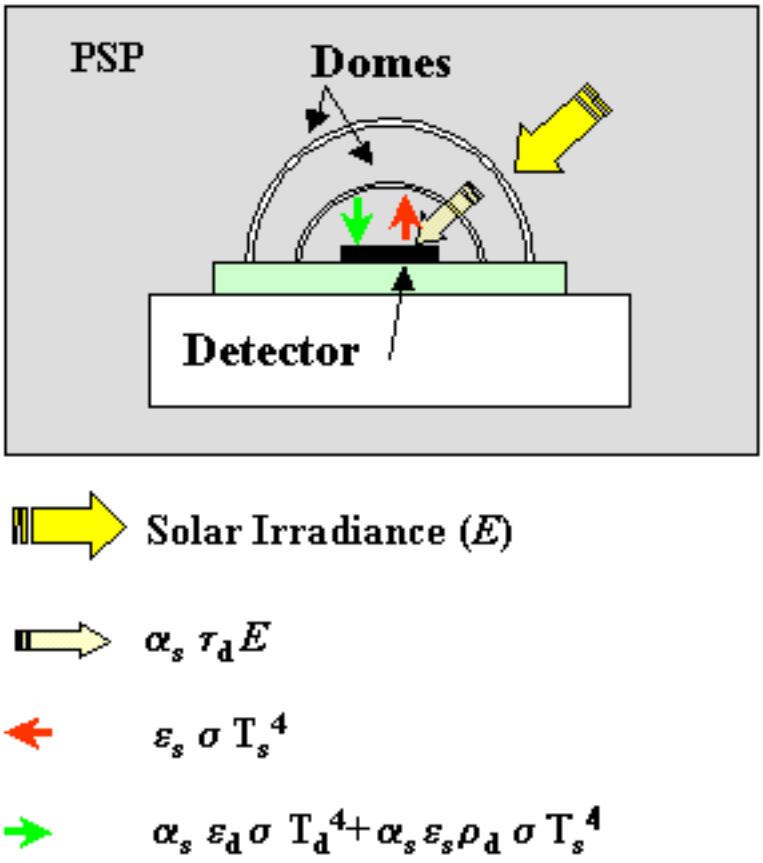

Figure 3.1: Location of the ARM sites. From the ARM web page

where T_s is the temperature of the sensor (hot junction of the thermopile), T_b is the temperature of the body of the instrument (cold junction of the thermopile), S is the Seebeck coefficient and C is the instrument sensitivity. Solving Equations 3.1 and Equation 3.2 for the solar irradiance E in terms of measurable variables yields,

$$E = U_e \left[\frac{S}{\alpha_s \tau_d c} + \frac{4\sigma S}{\tau_d}(1 - \varepsilon_s \rho_d) T_b^3 \right] + \frac{\varepsilon_s \sigma}{\tau_d}(\varepsilon_s T_b^4 - T_d^4) + \frac{\sigma}{\tau_d}(1 - \alpha_s) T_b^4, \tag{3.3}$$

where S is the Seebeck coefficient of the thermopile and U_e is the voltage output of the thermopile. The term $(\frac{\varepsilon_s \sigma}{\tau_d}(\varepsilon_s T_b^4 - T_d^4))$ corresponds to the thermal offset.

The term $\left[\frac{S}{\alpha_s \tau_d c} + \frac{4\sigma S}{\tau_d}(1 - \varepsilon_s \rho_d) T_b^3\right]$ corresponds to the proportionaly between the voltage output of the thermopile and the incident solar radiation. It is derived in the standard calibration process of the instrument in which the offset is assumed to be negligible. The term $(\frac{\sigma}{\tau_d}(1 - \alpha_s) T_b^4)$ can be neglected because the absorptivity of the detector

is close to 1 (0.98), hence it represents less than 5% of the thermal offset.

Finally Equation 3.1 can be simplified as

$$E = C_1 U_e + C_2 \sigma (T_b^4 - T_d^4), \tag{3.4}$$

which relates the incident solar irradiance to the output of the instrument and the thermal offset.

3.2 Nighttime Pyranometer Output

3.2.1 Zero Offset

The offset in radiometers due to thermal exchanges is often referred to as a zero offset because it becomes apparent when the signal should be zero due to the absence of solar radiation [27]. However it has been observed that the output from a PSP operating at night is typically non zero. PSP output during nighttime range from about 5 $\mathrm{W}m^{-2}$ to -10 $\mathrm{W}m^{-2}$ and can reach even -20 $\mathrm{W}m^{-2}$ when operating under some particular atmospheric and setting conditions. During nighttime, it is possible to keep track of the offset of a PSP because every signal different from zero comes from the thermal exchange between the dome and the body of the instrument. The challenge is to derive a relationship between measurable parameters and the instrument offset based on nighttime data, that can be applied during daytime.

3.2.2 Nighttime Correlation

On the format of the correlation

Dutton et al [5] suggest three possible ways to address the PSP thermal offset issue:

- Redesign the instrument to minimize the temperature gradient and the emissivity differences between the dome and the body of the PSP,
- Determine the temperatures of the dome and body compute the error term,
- Develop a quantitative surrogate for the error term using available data.

Although the second approach is considered difficult and even illusive by some [5], Bush et al [4] tried to characterize the offset by placing four thermistors in the instrument, two of them on the outside of the outer dome and the others two on the detector assembly. Bush et al. propose an algorithm to correct the offset as

$$Offset \propto \sigma(T_{od}^4 - T_s^4), \tag{3.5}$$

where σ is the Stefan-Boltzmann constant.

Haeffelin et al [13] and Smith [27] tried another approach to characterize the offset of the PSP. This new approach is based on the work of Bush et al. [4]. Using the fact that both inner and outer dome are coupled radiatively, Haeffelin et al. placed a thermistor on the inside of the inner dome and another one in the heat sink of the detector. This approach is based on three reasons [13]:

- The effective temperature of the inner dome can be monitored with a single thermistor.
- The relationship between the thermal offset and the inner-dome-to-body temperature difference holds even during large thermal shocks.
- The modified instrument is as rugged as a standard PSP, so it can be tested and operated in a large variety of environments.

Haeffelin et al. defines the offset as

$$Offset \propto \sigma(T_{id}^4 - T_b^4), \tag{3.6}$$

where σ is the Stefan-Boltzmann's constant.

The present work follows the approach proposed by Haeffelin et al. The PSP's used in this research were modified placing a thermistor on the inner dome and another one in the body of the instrument. The method described by Haeffelin et al. is preferred over that of Bush et al. due to the reasons reported above.

The first step in the research of the PSP thermal offset is to test Equation 3.6 during nighttime, that is, to analyze the zero offset.

Figure 3.2 shows the magnitude of the radiative exchange between the inner dome and the body (detector cold junction) versus the PSP output at night. The behavior of four PSP's, modified according to [13], PSP 30849 F3, PSP 31562 F3, PSP 27218 F3 and PSP 33028 F3 are shown in Figure 3.2 (a), (b), (c) and (d), respectively.

The nighttime output of the four PSP's presents a strong linear dependence on $\sigma(T_{id}^4 - T_b^4)$. This linear relationship can be expressed as

$$Offset = A\sigma(T_{id}^4 - T_b^4) + B, \tag{3.7}$$

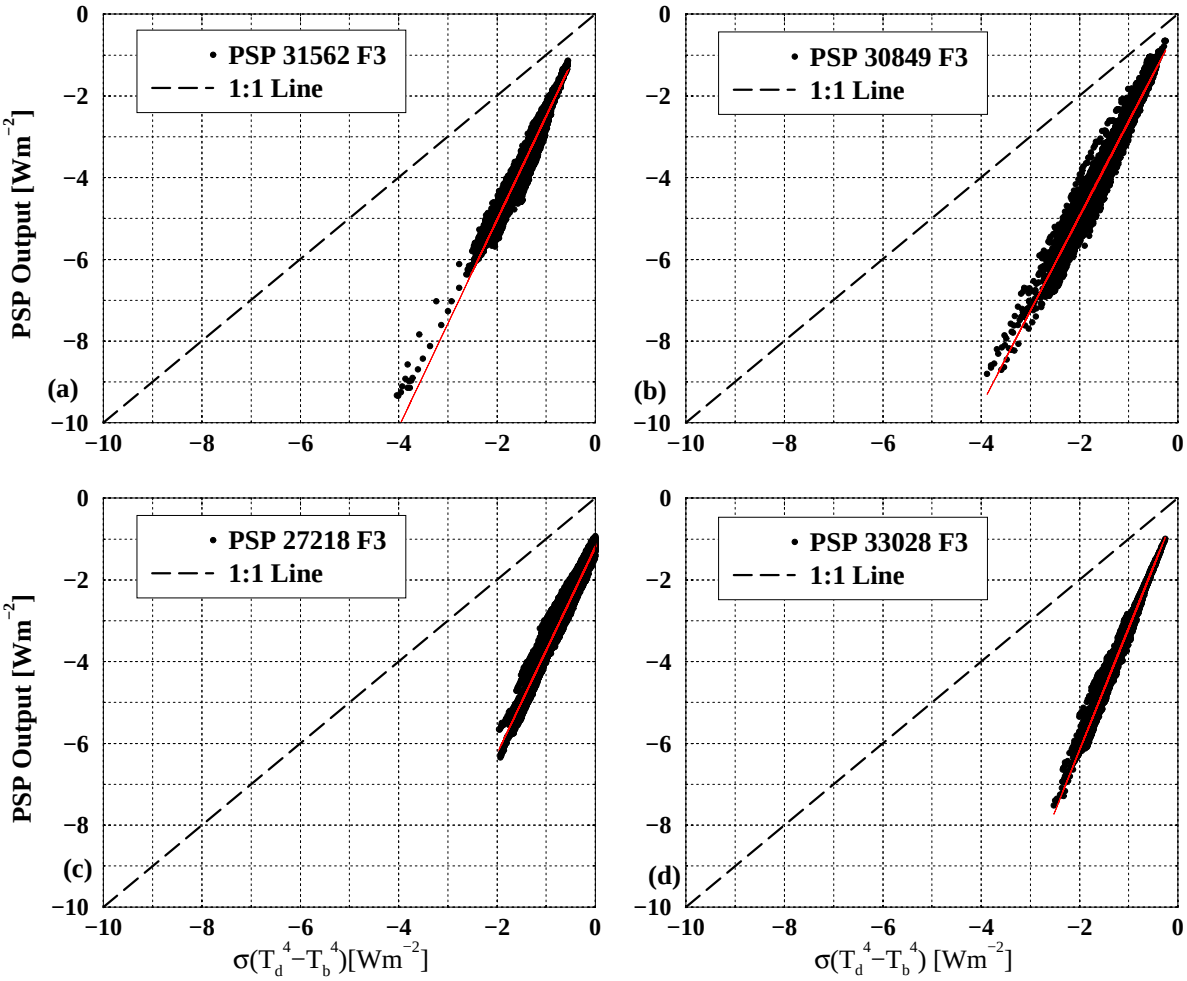

Figure 3.2: Theoretical blackbody radiative exchange between dome and detector versus PSP output at night for 4 different modified PSP's: (a) PSP 31562 F3, (b) PSP 30849 F3, (c) PSP 27218 F3 and (d) PSP 33028 F3.

where A and B are the slope and intercept coefficients regressed from the scatterplot of $\sigma(T_{id}^4 - T_b^4)$ versus PSP output at night.

Figure 3.2b, for example, shows a strong linear dependence of the nighttime output (thermal offset) with $\sigma(T_{id}^4 - T_{body}^4)$ following Equation 3.7. The red line shows a linear regression in which all the points of the data set have been included. This regression explains 97% of the variability of the output signal. The slope of the regression in Figure 3.2b is 2.32. A slope greater than 1 implies that the detector must lose heat through another form of heat transfer than radiation, or with another component than the inner dome. Haeffelin et al. [13] suggest that the inner dome is not completely opaque in the IR, so that the detector loses radiation to the outer dome as well. The regressions derived for each of the four PSP agree with the results from laboratory experiments made by Haeffelin et al. [13] when cooling or heating a modified PSP. Table 3.1 shows the slope,

intercept and regression coefficient (R^2) of the four regressions shown in Figure 3.2.

Instrument	Slope (-)	Intercept $[Wm^{-2}]$	R^2 (-)
PSP 31562 F3	2.53	0.05	0.98
PSP 30849 F3	2.32	-0.30	0.97
PSP 27218 F3	2.53	-1.19	0.98
PSP 33028 F3	2.99	-0.18	0.99

Table 3.1: Slope, intercept and regression coefficient (R^2) for PSP 30849 F3, PSP 31562 F3, PSP 27218 F3, PSP 33028 F3

On the accuracy of the nighttime correlation

Figure 3.3 shows the time series of PSP 31562 F3 and PSP 30849 F3 output for two consecutives nights in October 2000. The time is plotted in decimal fractions of the Greenwich Mean Time (GMT) which is five hours more than the Local Time (LT) of NASA LaRC (U.S. Eastern Standard Time). For example, 276.2 represents 4:48 am GMT on the day of the year 276 (2 October), or 11:48 pm LT on day 275. The output of PSP 30849 F3 is plotted in red and the output of PSP 31565 F3 is plotted in black. The offset for PSP 30849 F3 oscillate around -4 Wm^{-2} during both nights. The offset of the PSP 31562 F3, however oscillates around -2 Wm^{-2}. The difference is discussed later on. The light blue line represents the zero value. Zero or close to zero Wm^{-2} is the value that the output of the PSP's should be if the thermal offset were negligible.

The dark blue and green lines represent the value of the output of PSP 31562 F3 and PSP 30849 F3 after correction using Equation 3.7 and the coefficients given in Table 3.1. The value of the output of both PSP's after correction is reduced considerably. The mean offset is now about 0.25 Wm^{-2} and the large variability is completely removed.

Figure 3.4 is a barchart representing the accuracy of the correction during nighttime for PSP 30849 F3 and PSP 31562 F3, respectively. The data are from the LaRC data set and both instruments are operating on an Eppley tracker. The nighttime output is plotted in black for both instruments. The output of the instrument after correction is shown in red.

Table 3.2 shows the mean and standard deviation of the output of the two PSP's

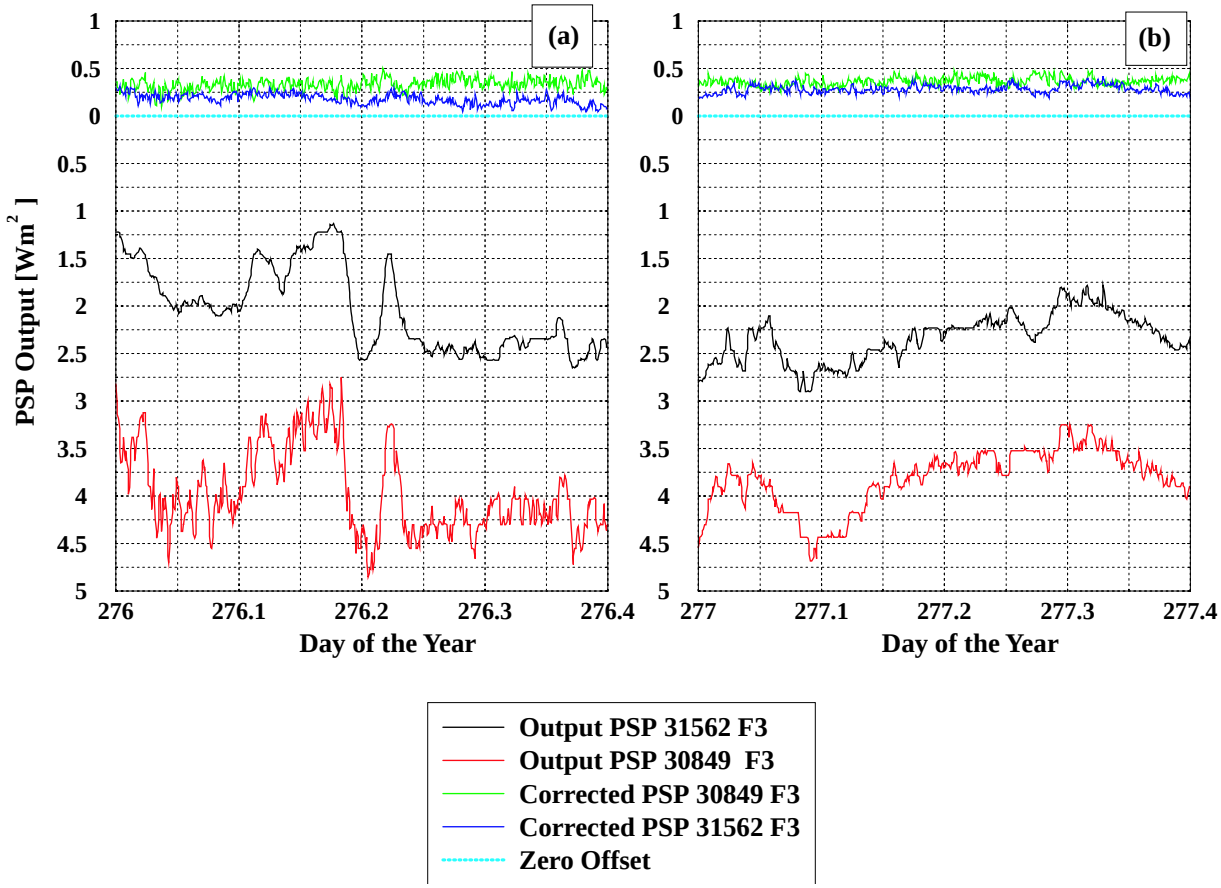

Figure 3.3: Time series of standard and corrected PSP output for (a) 2 October 2000 (day of the year 276) and (b) 3 October 2000 (day of the year 277).

at night before and after using the temperature-based correlation. The offset is virtually compensated, proving the validity of the correlation and correction method during nighttime.

Comparison with a B&W Pyranometer

The B&W PSP is an instrument that measures solar irradiance. However the design is completely different from the PSP. The thermal offset in the B&W is compensated (see chapter 2) and hence, theoretically, its thermal offset should be negligible when measuring diffuse irradiance.

Figure 3.5 and Table 3.5 compare the behavior of two modified PSP's and one B&W. Figure 3.3 shows pyranometer data for two nights during the month of March

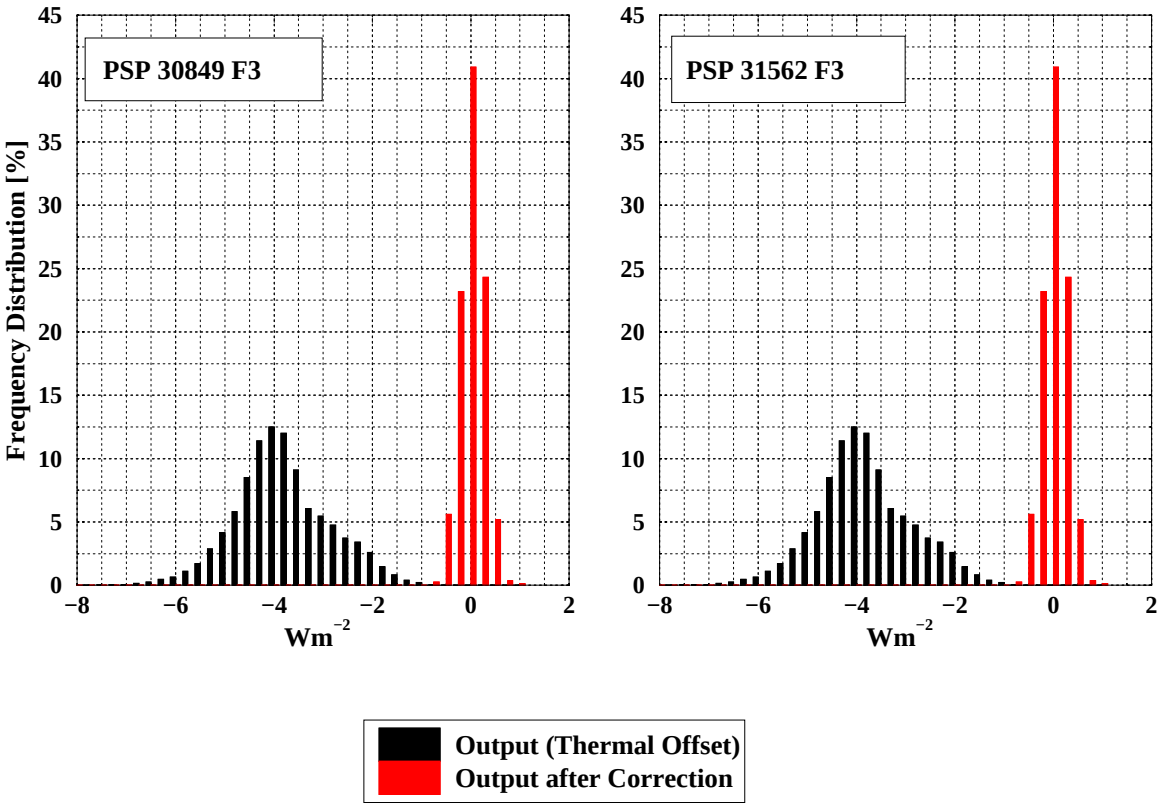

Figure 3.4: Distribution of thermal offset and corrected output for PSP 30849 F3 from September to December 2000(a) and PSP 31562 F3 from February to March 2001

2001. The output of PSP 30849 F3 and PSP 31562 F3 are plotted in red and black, respectively. The output of PSP 30849 F3 and PSP 31562 F3, after correcting their offset with Equation 3.7 are plotted in green and dark blue, respectively. The output of the B&W is plotted in magenta. During night 62 in Figure 3.3 the mean output of the PSP 30849 F3 is -3.31 Wm^{-2} but after correction the mean becomes -0.05 Wm^{-2} with a σ= 0.09 Wm^{-2}. The thermal offset is virtually removed. The behaviour of PSP 31562 F3 during the same night is very similar. The mean output is reduced from -3.13 Wm^{-2} to 0.03 Wm^{-2} with a σ= 0.05 Wm^{-2}.

Table 3.5 shows the mean and standard deviation of the nighttime output of PSP 30849 F3 and PSP 31562 F3 before and after correction and the nighttime output of a B&W pyranometer during two weeks in the month of March 2001. The thermal offset is virtually compensated for both PSP's and the mean value of the output of the PSP's after correction is close to the mean output of the B&W. The B&W shows virtually no offset at night as expected.

	Nighttime Output		Corrected Nighttime Output	
	Mean $[W/m^2]$	$\sigma[W/m^2]$	Mean $[W/m^2]$	$\sigma[W/m^2]$
PSP 30849 F3	-3.51	1.05	-0.10	0.24
PSP 31562 F3	-3.61	1.06	-0.02	0.18

Table 3.2: Average uncorrected and corrected nighttime offset for PSP 30849 F3 from September to December 2000 and PSP 31562 F3 from February to March 2001

	Output Uncorrected		Output Corrected	
	$\bar{x}$ [Wm^{-2}]	σ[Wm^{-2}]	$\bar{x}$ [Wm^{-2}]	σ[Wm^{-2}]
B&W	-0.01	0.08	N/A	N/A
PSP 30849 F3	-2.21	1.11	-0.04	0.22
PSP 31562 F3	-3.61	1.06	-0.02	0.18

Table 3.3: Comparison of the output of a B&W pyranometer and the uncorrected and corrected output of two PSP's, one of them installed on an Eppley tracker and the other mounted on a fix stand with different ventilation from February to March 2001

3.2.3 Variations of the Correlation on each Instrument

Figure 3.2 shows the temperature-based nighttime correlation for a data set that includes data points from September 2000 to December 2000. This data set contains a large amount of data points taken over a large variety of atmospheric conditions. This variety of atmospheric conditions gives a very good stability to the coefficients of the regression shows in Table 3.1

Table 3.4 shows the monthly values of the slope and intercept of the nighttime temperature-based regression for PSP 30849 F3. Table 3.4 shows the month, type of fan used for the ventilation of the instrument, number of days working with that type of ventilation and the values of the slope and intercept in the nighttime temperature-based regression. The monthly slopes are also stable on each ventilation system. The difference observed in November 2000 on the fix stand can be due to the particularity of the conditions during the short time period.

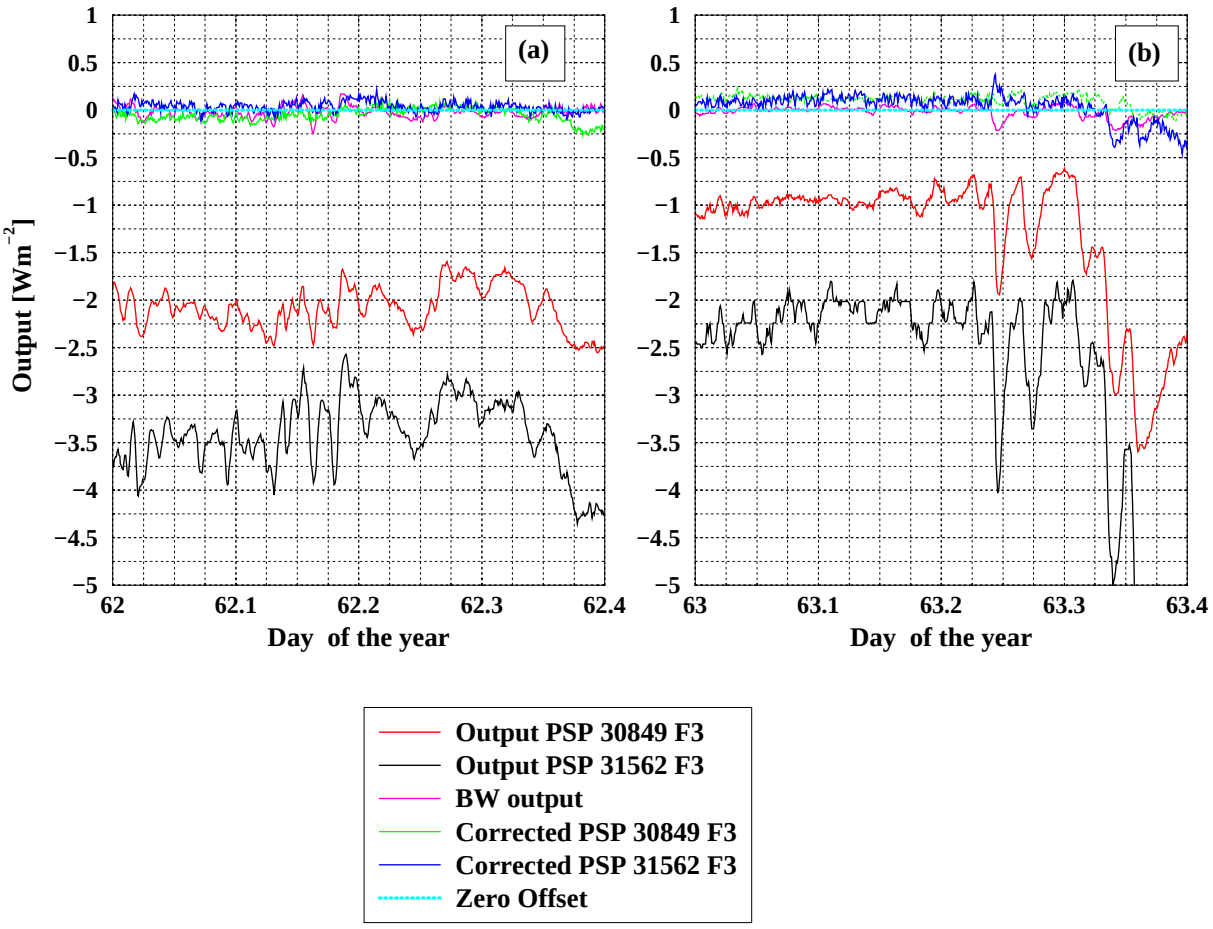

Figure 3.5: Comparison between the nighttime output of BW and modified PSP's on 3 and 4 March 2000, Day of the Year (DOY) 62-63

Table 3.5 shows the month-to-month values of the slope and intercept of the nighttime temperature-based regression for PSP 31562 F3. As for PSP 30849 F3 it presents a good monthly stability. However some perceptible variations in the slope exist between both instruments and for each instruments. These variations can be better appreciated in Figure 3.6 that shows the daily variation of the slope for PSP 30849 F3 from September to December 2000. The variation of the slope can be explained by four different effects:

- Homogeneous sky effect,
- Variation in the surface temperature,
- Thermistor location,
- Atmospheric conditions, such as rain.

Month	Fan	Number of days	Slope (-)	Intercept $[Wm^{-2}]$	Fan	Number of days	Slope (-)	Intercept $[Wm^{-2}]$
Sep 00	Tracker	22	2.33	-0.09	Fix stand I	0	—	—
Oct 00	Tracker	23	2.42	-0.16	Fix stand II	0	—	—
Nov 00	Tracker	15	2.39	-0.24	Fix stand II	7	2.86	-0.03
Dec 00	Tracker	13	2.47	-0.25	Fix stand II	17	2.57	-0.3
Jan 01	Tracker	0	—	—	Fix stand II	26	2.56	-0.26
Feb 01	Tracker	0	—	—	Fix stand II	28	2.56	-0.15
Mar 01	Tracker	0	—	—	Fix stand II	14	2.53	-0.17

Table 3.4: Variability of the regression coefficients of Equation 3.7 from September 2000 to March 2001 for PSP 30849 F3.

Homogeneous Sky Temperature Effect

The low thermal conductivity of the dome of the PSP is one of the causes of the thermal offset. The low thermal conductivity creates a temperature gradient in the dome. Smith [27] proved that under homogeneous irradiance conditions the blackbody temperature of the dome can be determined by a single thermistor located half-way between the base and the tip of the dome. However when the surrounding radiative field is not homogeneous or when the dome is radiating to a non-homogeneous temperature media, the temperature distribution inside the dome will vary from the homogeneous condition case. Therefore the measured temperature will not represent the mean blackbody emission temperature. This shortcoming will introduce variability in the slope.

Figure 3.7 shows the evolution of the slope of PSP 30849 F3, PSP 31562 F3 and PSP 33028 F3 over a two-week period. PSP 33028 F3 is mounted on an Eppley tracker. PSP 30849 F3 and 31562 F3 are mounted on a fix stand. During nighttime the thermistor of PSP 33028 F3 is oriented towards the South. The thermistors PSP 30849 F3 and PSP 31562 are facing the North. The slopes of PSP 31562 F3 and PSP 30849 F3 are correlated at all times, as expected. The slopes of PSP 33028 F3 are close to the monthly mean values on the same nights than the other 2 PSP's. When the slopes of PSP 30849 F3 and PSP 31562 F3 deviate from the mean, that of PSP 33028 also deviates but in the other direction, as seen on 12/23/2000 and 12/25/2000 as shown in Figure 3.7. This is due

Month	Fsn	Number of days	Slope (-)	Intercept $[Wm^{-2}]$	Fan	Number of days	Slope (-)	Intercept $[Wm^{-2}]$
Sep 00	Tracker	0	—-	——	Fix stand I	22	2.42	0.03
Oct 00	Tracker	0	—-	——	Fix stand II	25	2.76	0.32
Nov 00	Tracker	0	—-	——	Fix stand II	24	2.69	0.16
Dec 00	Tracker	4	2.80	0.31	Fix stand II	27	2.70	0.16
Jan 01	Tracker	11	2.67	0.14	Fix stand II	15	2.64	0.1
Feb 01	Tracker	21	2.53	0.09	Fix stand II	0	—-	—-
Mar 01	Tracker	14	2.62	0.21	Fix stand II	0	—-	—-

Table 3.5: Variability of the regression coefficients Equation 3.7 from September 2000 to March 2001 for PSP 31562 F3.

to the difference in orientation of the thermistors at night (South sky versus North sky). The red and orange lines corresponding to PSP 31562 F3 and PSP 30849 F3, respectively, are always correlated during this period of time, however, PSP 33028 F3 is not.

Ventilation Effect

Pyranometers are mounted on a platform. A fan is attached under this platform. The mission of the fan is to blow ambient air (in some cases preheated air) over the body and dome of the instrument to create a more isothermal environment and reduce the offset. Two types of fans have been used, a tracker fan and a fix-stand fan. The tracker fan is less efficient than the fix-stand because of restricted air flow. Tables 3.4 and 3.5 show a variation of 4% in the slope for both instruments depending on the type of fan used. Besides the monthly slopes are more stables when an fix-stand fan is used because of the greater flow rate.

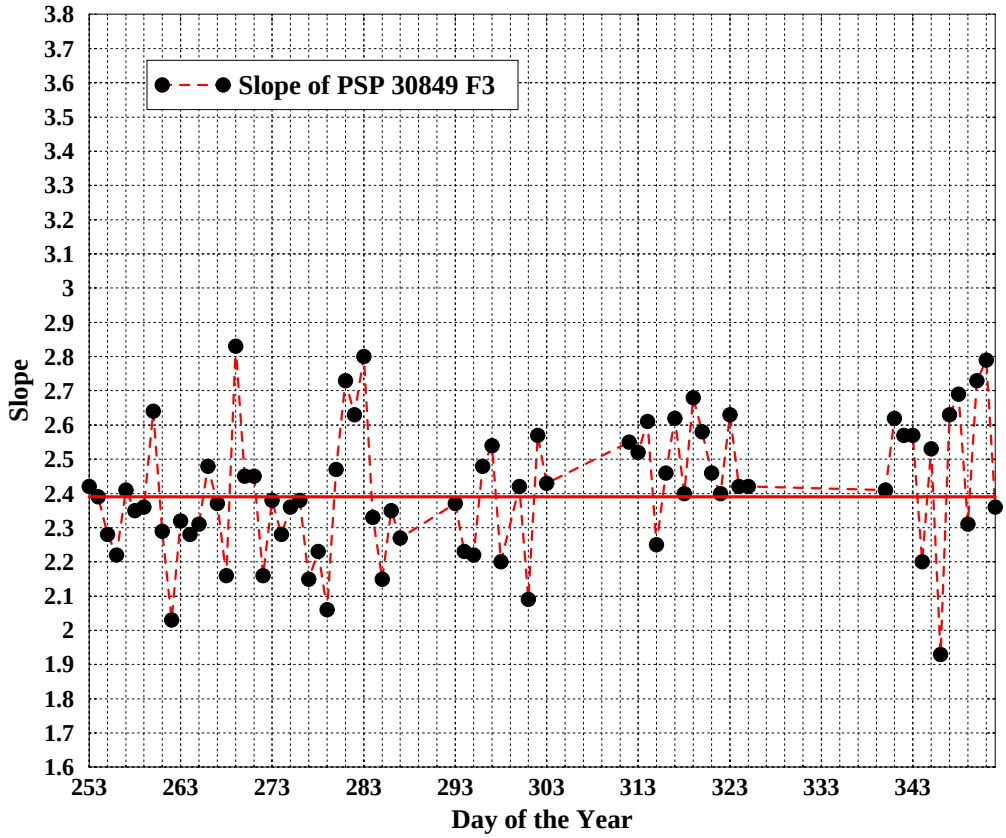

Figure 3.6: Daily variations of the slope for PSP 30849 F3 from September 9 2000 to December 18 2001

Atmospheric condition and thermistor placement

Installing the thermistor on the surface of the inner dome is a delicate and difficult task. As a result, the actual location of the dome thermistor vary somewhat from one instrument to the next. If the thermistor is moved a few degrees from its ideal point the measured temperature is going to deviate from the ideal which will modify the slope of the correlation. This is another reason for the variation of the slope from instrument to instrument.

Atmospheric conditions can modify the slope, in particular rain, snow and dew. The drops on the dome and their distribution produce a non-homogeneous dome temperature. This non-homogeneous distribution of the the dome temperature differs from the homogeneous one for what the thermistor measures a representative temperature. The effect is similar to the one produced by a non-homogeneous sky temperature.

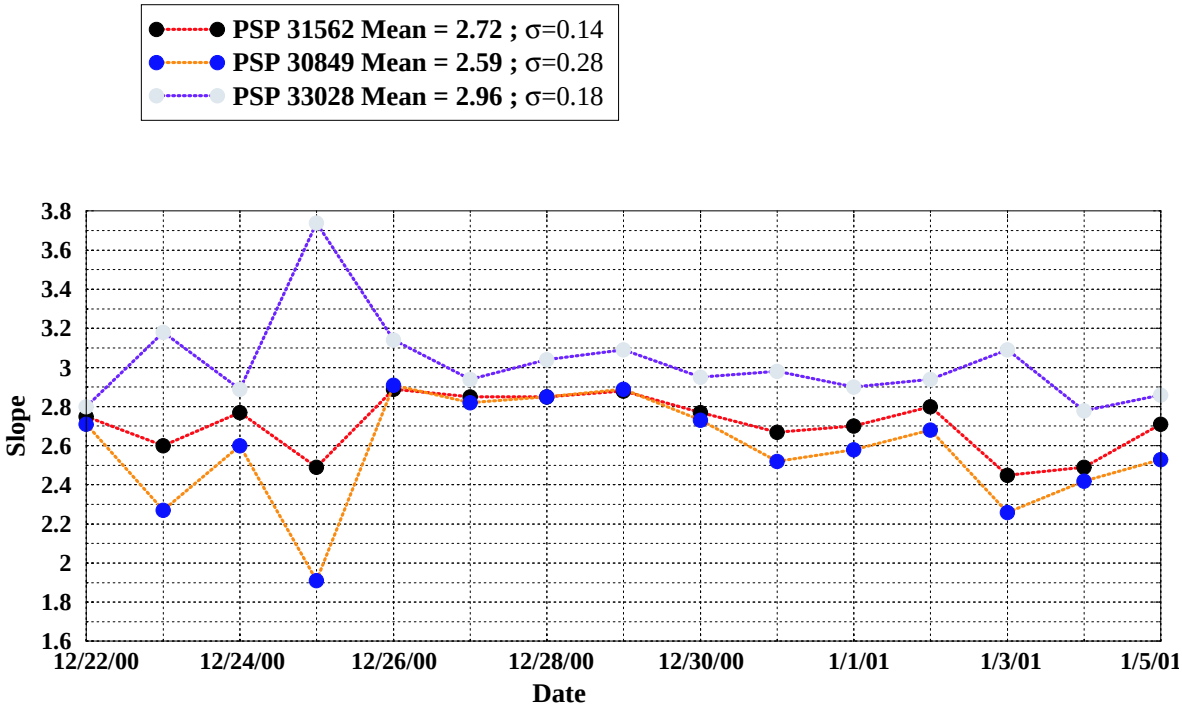

Figure 3.7: Variation in the slope with the homogeneity of the sky from 20 December 2000 to 5 January 2001.

3.2.4 Statistical Analysis

Variation of the nighttime slope in one instrument

Figure 3.6 shows the daily average of nighttime slopes for PSP 30849 mounted in an Eppley tracker from September 9 2000 to December 18. Table 3.6 summarizes the statistical variables of the population analyzed. The mean of the slope for Equation 3.7 is 2.412 and the standard deviation σ is 0.191. For a clear sky day with a thermal offset of 12 Wm^{-2} the corresponding is about $\sigma(T_d^4 - T_b^4)$ of around 5 Wm^{-2}. An uncertainty of $\pm$ 0.2 in the slope will produce an uncertainty in the offset estimate of $\pm$ 9%. From this data set it is not possible to make a more extensive data analysis because the samples of the population are not independent. The slope depends on the atmospheric conditions, so the slope of day "d" cloud be related to the slope of day "d-1".

In order to increase the accuracy of the correction of the thermal offset it is recommended derive the coefficients of Equation 3.7 using at least two weeks and preferably one month data. Table 3.1 shows the coefficients of Equation 3.7 applied at night for 4 different instruments. Each regression is made with at least one month of data. From all

Mean	2.41
Standard Error	0.02
Standard Deviation	0.19
Variance	0.04
Observations	72
Minimum Value	1.93
Maximum Value	2.83

Table 3.6: Statistical variables of the nighttime slope of Equation 3.7 from September 2000 to December 2000 for PSP 30849 F3 from Figure 3.6.

these four different instrument it can be concluded that when the amount of data points used to derive the coefficient of Equation 3.7 exceed one month the correlation coefficient R^2 is close to 1. Therefore more than 97% of the variation in the slope is explained by the regression.

Variation of the slope among instruments

The purpose of this section is to find out if the regression slopes (Equation 3.7) for two different PSP's are significantly different. Table 3.8 shows the monthly slopes for two different cases, one where both instruments are working on an Eppley tracker and the other one where both instruments are working on a fix stand. To find out if the slopes for PSP 30849 F3 and PSP 31562 F3 are significantly different a test of hypothesis is done on both populations. The null hypothesis is in both cases $H_0 : \mu_1 - \mu_2 = 0$. If the null hypothesis is true, then the following statistical test must be accomplished:

$$t = \frac{\mu_1 - \mu_2}{S_p \sqrt{\frac{1}{n_1} - \frac{1}{n_1}}} \leq t_{\alpha,df} \tag{3.8}$$

where t is the the value of a t distribution S_p is the standard deviation of the population, μ is the mean of the population, α is the level of confidence and df are the degrees of freedom. Table 3.7 summarizes the results of the test of hypothesis given in Equation 3.8 stating that the slopes are identical for both instruements.

This statistical test proves that with a 95% confidence the slopes of two different

	Tracker	Fix stand
$t_{\alpha,df}$	2.15	1.94
α, df	0.05, 5	0.05, 6
t	4.22	9.55
Null Hypothesis	False	False

Table 3.7: Summary of a test of hypothesis to compare the difference in slope for PSP 30849 F3 and PSP 31562 F3.

instruments in two different ventilation condition are significantly different and no universal coefficient that can be applied to all the instrument. However the difference in the mean slope for both instrument is around 0.2. So if the slope derived for one instrument is applied to the other the resulting error in the predicted offset will be around 9%.

Ventilation	PSP30849F3	PSP31562F3	Ventilation	PSP30849F3	PSP31562F3
Tracker	2.33	2.67	Fix stand II	2.57	2.64
	2.42	2.53		2.56	2.76
	2.39	2.62		2.56	2.69
	2.47	—-		2.53	2.70

Table 3.8: Nighttime slope for Equation 3.7 for PSP 30849 F3 and PSP 31562 F3 mounted on a tracker and on a fix stand.

Variation of the slope with ventilation

The purpose if this section is to determine if the slope of Equation 3.7 derived at night is significantly different under two ventilation conditions. Table 3.10 shows slope data from Table 3.4 and Table 3.5. To test if the slopes are significantly different with a 95% confidence, data from two different PSP's are analyzed (PSP 30849 F3 and PSP 31562 F3). Table 3.10 shows the values of monthly slopes of Equation 3.7 for both instruments in two ventilation conditions: working on an Eppley Tracker and on a fix stand. A test

of hypothesis on these data for both instruments is done. The null hypothesis in both cases is: $H_0 : \mu_1 - \mu_2 = 0$. If that is true then, the following statistical test must be accomplished:

$$t = \frac{\mu_1 - \mu_2}{S_p \sqrt{\frac{1}{n_1} - \frac{1}{n_1}}} \leq t_{\alpha,df} \tag{3.9}$$

where t is the the value of a t distribution, S_p is the standard deviation of the population, μ is the mean of the population, α is the confidence and df are the degrees of freedom. Table 3.9 summarizes the results of the test of hypothesis stating that the two ventilation systems produce identical slopes.

	PSP 30849 F3	PSP 31562 F3
$t_{\alpha,df}$	1.943	2.01
α, df	0.05, 6	0.05, 5
t	4.93	2.26
Null Hypothesis	False	False

Table 3.9: Summary of a test of hypothesis to compare the dependence of ventilation on the slope of two instruments: PSP 30849 F3 and PSP 31562 F3.

This statistical test proves that with a 95% confidence the slopes of a particular instrument under two different ventilation conditions are significantly different, therefore the slope is dependent on the ventilation.

3.2.5 Conclusions

The thermal offset is a function of several variables:

$$Offset = f(Instrument, Ventilation, Atmospheric\ \ Conditions), \tag{3.10}$$

It has been proven that the nighttime slope of Equation 3.7 depends on the instrument, mainly because of the complexity of the installation of the thermistor. The slope depends also on the ventilation which creates a more isothermal environment and on the atmospheric conditions that modify the temperature gradient in the dome of the instrument and alter the reading of the thermistor. Therefore in order to calculate the most representative slope to retrieve the offset it is suggested to regress the coefficient of Equation 3.7 for each instrument in each site in each ventilation condition and over two weeks to one month of data.

PSP 30849 F3		PSP 31562 F3	
Fix Stand	Tracker	Fix Stand	Tracker
2.57	2.33	2.76	2.67
2.56	2.42	2.69	2.53
2.56	2.39	2.70	2.62
2.53	2.47	2.64	—-

Table 3.10: Nighttime slope for Equation 3.7 for PSP 30849 F3 and PSP 31562 F3 mounted on a tracker and on a fix stand.

3.3 Daytime Thermal Offset

3.3.1 Characterization

To characterize the thermal offset of a PSP during daytime is a much more complex task than to correct the zero offset. The output signal of a PSP during daytime is made of two different signals,

$$OutputSignal = TrueE + \Sigma Errors, \tag{3.11}$$

the signal due to the true irradiance incident on the instrument and the signal coming from the sum of errors due to the uncertainty in the measurements. The thermal offset is the predominant error for a pyranometer shaded from the direct solar beam. The challenge here is to separate the signal due to the solar irradiance from the errors. There are three possible methods to separate and characterize the offset during daytime:

- Using thermistors as done during nighttime,
- Periodically shading the PSP from all solar radition to record the offset signal (capping),
- Comparing the output of a regular PSP with a B&W

The present work uses thermistors installed in PSP's as a method to characterize the thermal offset. Results are validated by comparison with capping output and B&W

irradiances. The use of thermistors to characterize the offset, is considered in this research as more accurate than the comparison between a PSP and a B&W. The time constant of the detector of the B&W is slower than that of a PSP, so under variable cloudiness the PSP-B&W difference can be quite noisy. In addition differences could also be attributed to other instrument characteristics than thermal offset, such as calibration uncertainty.

The procedure used to characterize and correct the offset with temperature measurements during the daytime is similar to the nighttime procedure described in section 3.2. The thermistors placed in the dome and body of the PSP record the temperature gradient of the instrument. The daytime offset is due to the same infrared radiative exchange that occurs at night. Therefore Equation 3.7 with coefficients A and B found at night should still apply.

3.3.2 Validation of the Nighttime Correlation during daytime

Two possible methods can be used to validate the nighttime correlation during daytime: the capping method and the comparison of the output signal of the PSP with the output signal of a B&W, as discussed below.

Capping Method

Gulbrandsen [10] suggests an experiment to derive the offset signal from the measurements when the PSP is working during daytime. The method takes advantage of the fast response of the thermopile of the instrument. The main objective of the experiment is to simulate nighttime conditions (absence of solar irradiance) during daytime. Under these conditions the output of the instrument is the thermal offset.

A cap is used to shade the dome and the detector from all solar radiation. The cap is made of white plastic and is coated on the inside with a infrared reflecting material. The inner diameter of the cap is the same as the diameter of the outer dome of the PSP. Figure 3.8 shows a capping experiment at the radiometric site at NASA LaRC

Figure 3.9 shows the PSP signal versus time during a capping experiment on two different PSP's; PSP 31562 F3 is shown in black and PSP 30849 F3 in red. The capping experiment was conducted on day 85 2001 at a time close to solar noon, in clear sky conditions. The pink vertical line shows the beginning of the capping procedure, that is when the cap is placed on top of the dome. The temperature-based offset of PSP 31562 F3 is plotted in green and the temperature-based offset of PSP 30849 F3 is plotted in blue. Each time step in the experiment corresponds to two seconds. The cap is placed above on top of the dome at time step 25, that is 50 seconds after the beginning of the experiment.

Figure 3.8: Capping experiment at the radiometric site at NASA LaRC. Note that both PSP's are placed on an Eppley Solar Tracker. Both instruments are measuring diffuse irradiances. The dome and detector of the PSP on the right are capped, however, the PSP on the left is not. The disk of the solar tracker shades the domes and detector of the PSP.

The first step is to calculate the time constant of both Eppley PSP's based on Figure 3.9. This was a very delicate calculation because the time constant for both instrument is on the order of 2 seconds, which is the time step. In order to estimate the thermal offset at a time $t = t_0$(step 25 in Figure 3.9) the dome of the PSP is capped, shading the detector from all solar radiation. However the IR exchange between the dome and the detector, which is the cause of the thermal offset, remains unchanged. The output of the thermopile is then driven solely by the exchange of IR. Due to the fast response of the thermopile, the output of the instrument will rapidly follow the IR exchange. The IR exchange can be considered constant and equal to the IR exchange prior to capping during at least 30 sec, after that the dome starts to reach the radiative equilibrium with the body of the instrument.

A thermopile with a time constant on the order of 1-2 seconds reaches 99.99% of a steady-state output within 10-12 sec. The true thermal offset a time $t = t_0$ is defined as the 10-sec average of the signal produced by the thermopile from $t = t_0 + 10$ sec to $t = t_0 + 20$ sec. The estimate of the thermal offset at a time $t = t_0$ based on temperature measurements is defined as the 10 sec. average of the offset at a time $t = t_0 - 10$ to $t = t_0$.

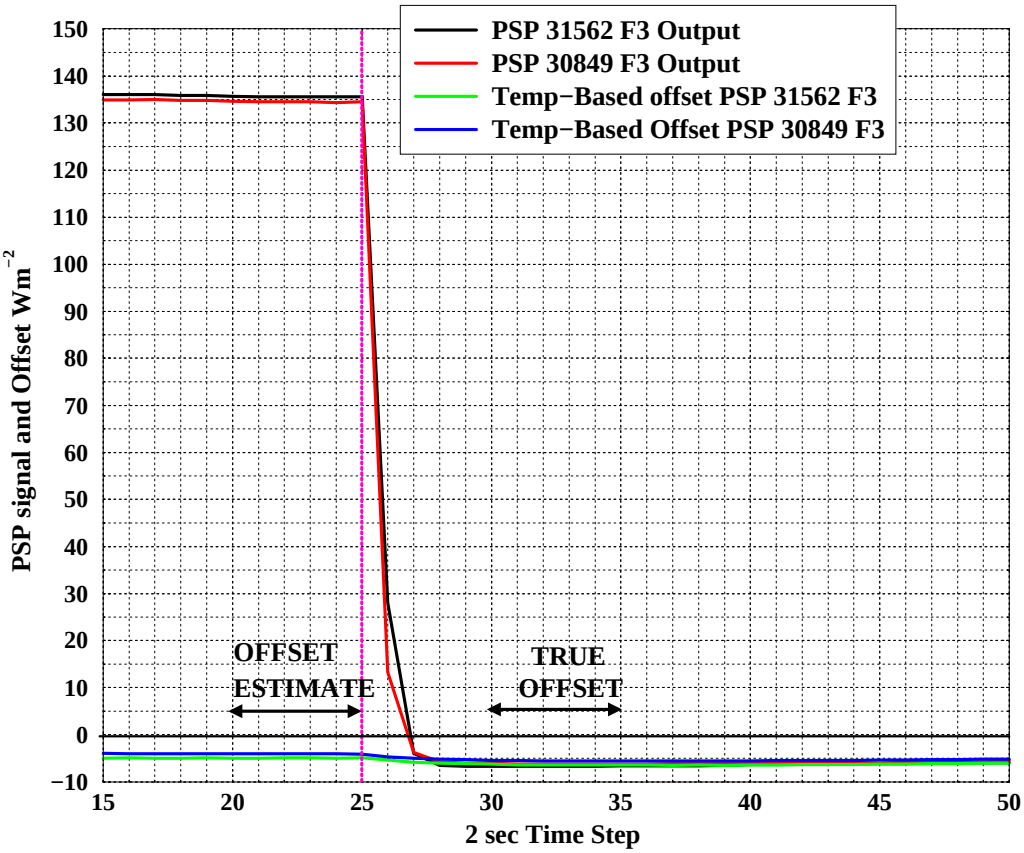

Figure 3.9: Capping experiment on PSP 30849 F3 and PSP 31562 F3. The data are recorded with a 2-sec time step

The 10-sec average is used to remove some noise from the data.

Table 3.11 summarizes the results of the cappings shown in figure 3.9. The temperature based offset estimate using the temperature correlation derived at night are 4.08 Wm^{-2} and 4.95 Wm^{-2} for PSP 30849 F3 and PSP 31562 F3, respectively. After capping the output of PSP 30849 F3 and PSP 31562 F3 are 6.26 Wm^{-2} and 6.61 Wm^{-2}, respectively. The offset is underestimated using the nighttime temperature-based regression.

To analyze the nature of this difference a whole set of cappings over very different atmospheric condition were performed on PSP 30849 F3 and PSP 31562 F3. We define the offset estimate error as the difference between the temperature-based offset before capping and the output of the PSP after capping. Figure 3.10 is a scatterplot of the offset estimate error versus the output of the PSP before capping. The data for PSP 30849 F3 and PSP 31562 are plotted in black and red, respectively. Figure 3.10 shows a square root dependence of the offset estimate error with the amount of irradiance arriving at the detector. Although the thermistor mounted on the dome is painted white and its mass is negligible compared to the mass of the dome, the temperature of the thermistor increases

	Estimated Offset $(t_0 - 10)$ to t_0 $[\mathrm{W}m^{-2}]$	Output $(t_0 + 10)$ to $(t_0 + 20)$ $[\mathrm{W}m^{-2}]$
PSP 30849 F3	-4.08	-6.26
PSP 31562 F3	-4.95	-6.61

Table 3.11: Comparison between the temperature-based offset estimate before capping the dome and the output of the PSP after capping

due to absorption of solar radiation. Equation 3.7 can be modified to take into account the effect of solar irradiance on the thermistor as

$$Offset = A\sigma(T_d^4 - T_b^4) - C\sqrt{E} + B, \tag{3.12}$$

where E is the diffuse irradiance measured by the PSP, T_d and T_b are the temperatures of the dome and body of the instrument, respectively, A and B are the regression coefficients of Equation 3.7 and C is a regression coefficient derived from Figure 3.10.

Comparison with a B&W Pyranometer

The other method to validate the temperature-based offset is to compare the output of the PSP to that of a B&W pyranometer. The B&W is designed to minimize the thermal offset (see chapter 2). However the response of a B&W pyranometer to transient processes is completely different from the one of a standard PSP. In order to make an appropriate comparison of the output of both instruments it is necessary to analyze the response of both instruments. The time constant τ is usually defined as the time that a dynamic process takes to complete (1-e^{-1})% (63.2%) of the process. The time constant gives information on how fast the response of the instrument is. The 95% and 99.99% response are other two widely used parameters to characterize the response of an instrument. They refer to the time the instrument takes to reach 95% and 99.99 %, respectively, of the steady state value.

Figure 3.11 shows a response of PSP 31562 F3 and B&W 32954 during a capping experiment. Under cloudy sky or broken cloud conditions the amount of irradiance reaching the detector can vary rapidly. The discrepancy in time constant becomes apparent when plotting the difference between the output of a PSP and a B&W operating side by side. Under clear skies the solar irradiance changes slowly and the time constant becomes less of a limiting factor.

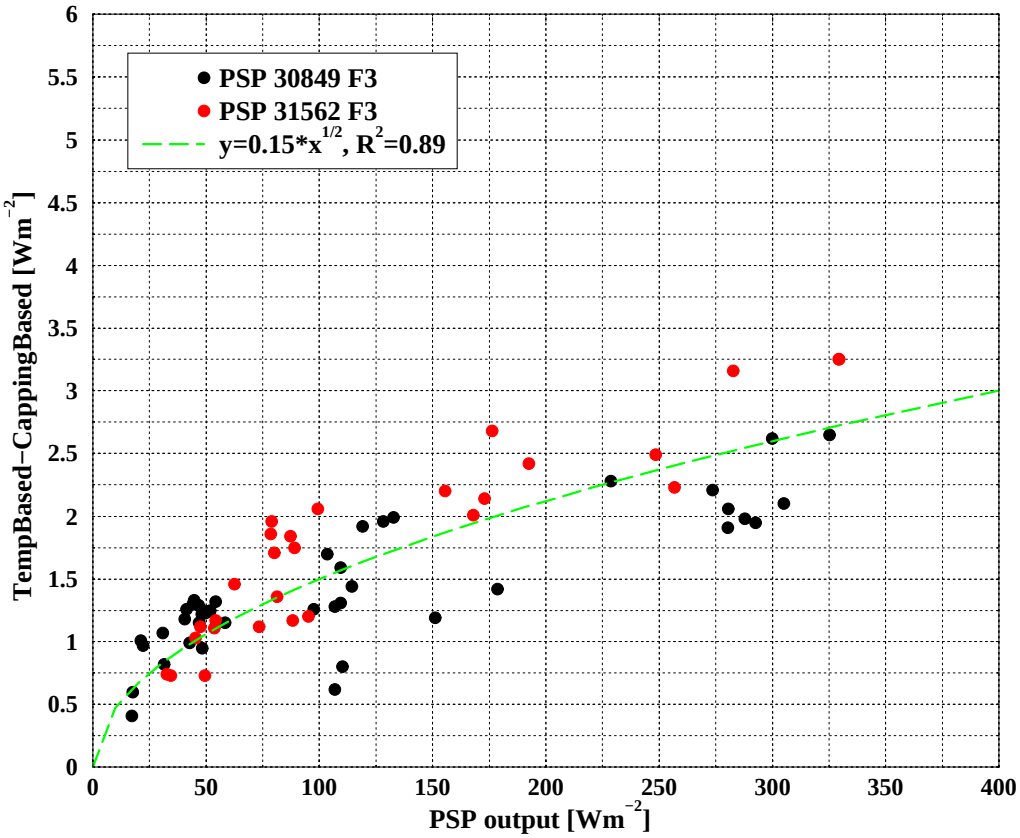

Figure 3.10: Capping experiments on PSP 31562 F3 and 30849 F3

Figure 3.12 shows the response of B&W 32954 during an extended capping experiment. The experiment was conducted under clear sky conditions. Initially the output of the B&W is constant, the small decrease around time step 140 is due to the reflection of the solar radiation when approaching the instrument. The dome of the B&W is capped 20 seconds after the approach. The instrument takes more than 50 times steps (more than 1 minute and a half) to reach steady state. Table 3.12 shows the 1/e, 95% and 99.99% responses for a regular PSP and a B&W based on Figure 3.11 and 3.12. A regular PSP responds much faster than a B&W to sudden changes in the solar irradiance. A regular PSP takes around 6 seconds to reach the steady state whereas a B&W takes more than 2 minutes to reach steady state. Based on this results the data is average over 15-min intervals to compare the measurements of both instruments. Fifteen minutes is long enough to remove the effect of the difference in time response of the measurements.

Figure 3.13 (a) shows the difference between the output of PSP 31562 F3 and B&W 32954 versus the output of the PSP for all sky conditions and clear sky days plotted in black and blue, respectively. A linear regression is fitted on the all-sky conditions data set. This regression shows a calibration problem between PSP 30849 F3 and B&W 32954 of around 3%. However for clear skies the agreement between both instruments is fairly

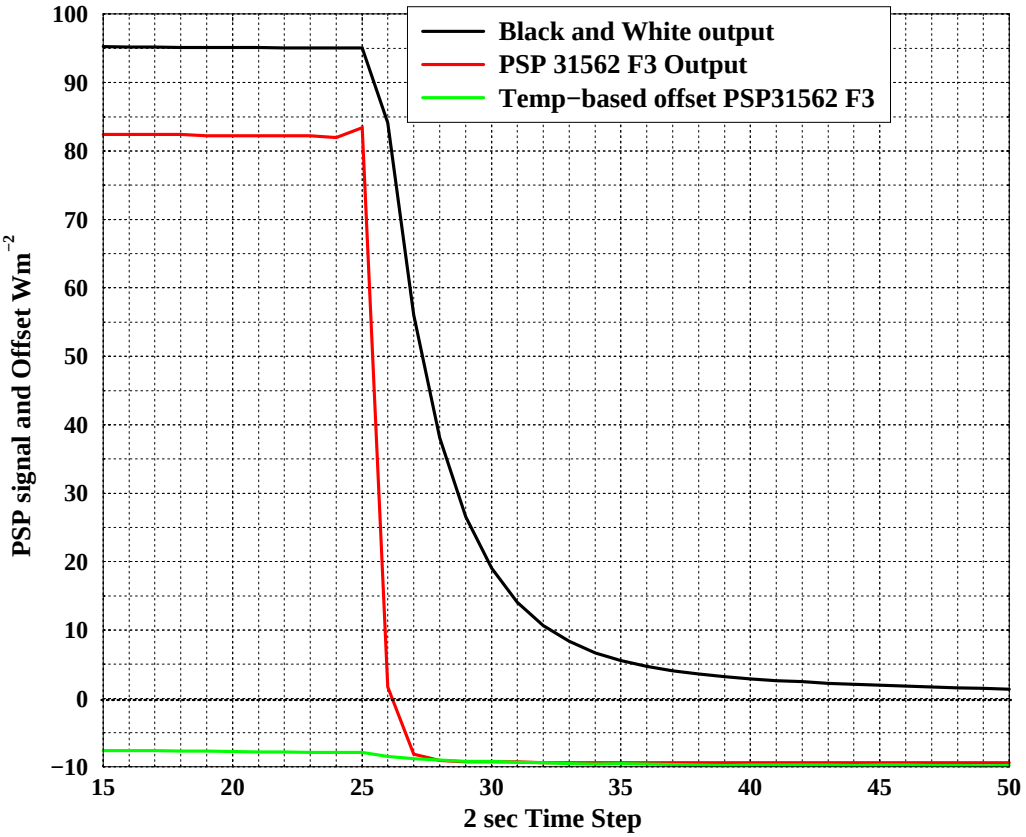

Figure 3.11: Capping experiment on a PSP and a B&W pyranometer

good. The mean of the difference between the B&W output and the corrected PSP is close to zero ($\bar{x} = -0.21 Wm^{-2}$) with a standard deviation of $2.21 Wm^{-2}$.

3.4 Summary and Conclusions of the Chapter

It has been proven that the offset of PSP's can be characterized using thermistors placed on the dome and in the body of PSP's. These thermistors keep track of the temperature gradient between dome and body, which is the cause of the thermal offset. A general correlation to retrieve the offset during daytime and nighttime has been found

$$Offset = A\sigma(T_d^4 - T_b^4) - B\sqrt{E} + C, \tag{3.13}$$

Coefficient A, B and C must be found for every instrument, ventilation conditions and location to optimize the correction.

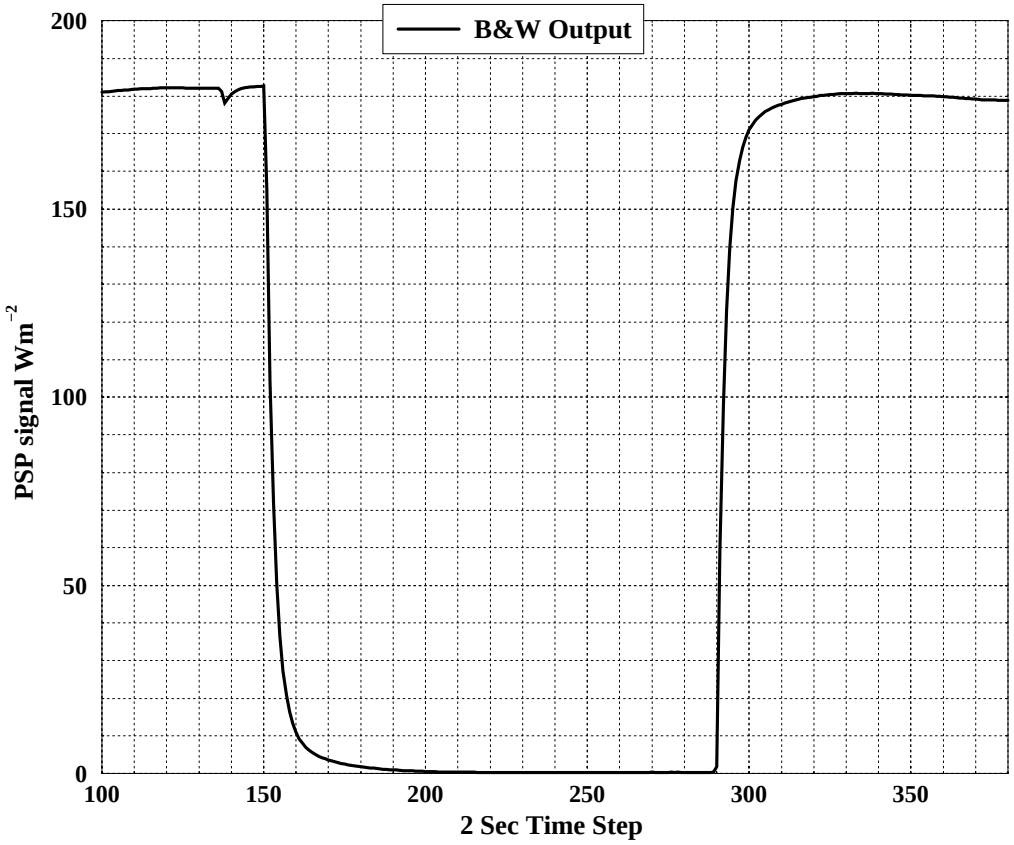

Figure 3.12: Capping experiment on a B&W pyranometer to determine the time constant

τ	PSP	B&W
(1-e^{-1})	1-2 sec	5 sec
95%	2-4 sec	22-24 sec
99.99%	10-12 sec	2 min 30 sec- 2 min 40 sec

Table 3.12: Comparison between the time constants (τ=(1-e^{-1}),$\tau = 95\%$,$\tau = 99.99\%$) of a regular PSP and a B&W

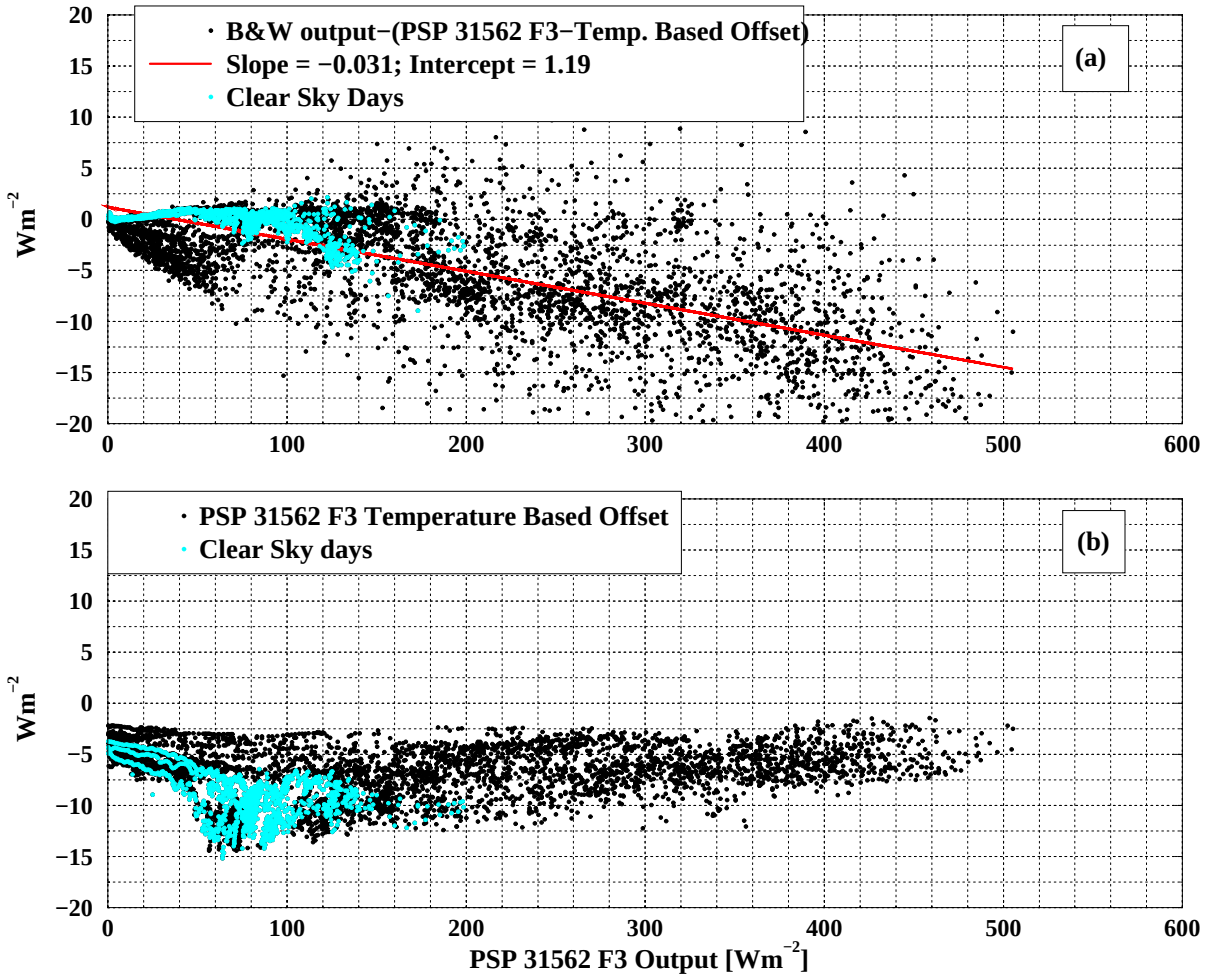

Figure 3.13: (a)Difference between the B&W signal and the temperature based corrected output of a PSP and (b) temperature-based offset of a PSP